Available online at www.sciencedirect.com

ScienceDirect
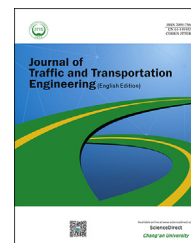
Original Research Paper

Chemical, morphological and rheological characterization of bitumen partially replaced with wood bio-oil: Towards more sustainable materials in road pavements

Lorenzo Paolo Ingrassia [a,*], *Xiaohu Lu* [b], *Gilda Ferrotti* [a], *Francesco Canestrari* [a]

[a] *Dipartimento di Ingegneria Civile, Edile e Architettura (DICEA), Università Politecnica delle Marche, Ancona 60131, Italy*
[b] *Nynas AB, Nynäshamn SE-14982, Sweden*

HIGHLIGHTS

- Additional functional groups related to esters appear for the bio-binders.
- Bio-binders show reduced saturates, aromatics and asphaltenes, as well as increased resins.
- No phase separation is observed from the microscopic analysis.
- Temperature susceptibility is not negatively affected by the bio-oil.
- The bio-binders may have improved low-temperature and fatigue behaviour.

ARTICLE INFO

ABSTRACT

Nowadays, sustainability and circular economy are two principles to be pursued in all fields. In road pavement engineering, they can be put into practice through the partial substitution of bitumen with industrial residues and by-products deriving from renewable materials. Within this framework, this paper presents an extensive investigation of the chemical, morphological and rheological properties of bio-binders obtained by mixing a conventional 50/70 bitumen with different percentages by weight (0, 5%, 10% and 15%) of a renewable bio-oil, generated as a residue in the processing of wood into pulp and paper. Results show that overall the bio-oil provides a softening effect, which, in terms of performance, leads to an improvement of the low-temperature behaviour and fatigue resistance with respect to the control bitumen, in spite of an increased tendency to permanent deformation. Although no chemical reaction appears to occur after blending, the peculiarities of the bio-oil affect the chemistry of the resulting bio-binders, whereas no phase separation is observed from the microscopic analysis. In addition, a Newtonian behaviour, an unchanged temperature susceptibility and a good fitting of 1S2P1D model to the rheological data are found, regardless of the bio-oil percentage considered. These promising outcomes suggest that such bio-binders can be favourably employed for several applications in road pavements.

* *Corresponding author*. Tel.: +39 071 220 4780; fax: +39 071 220 4780.
E-mail addresses: l.p.ingrassia@pm.univpm.it (L.P. Ingrassia), xiaohu.lu@nynas.com (X. Lu), g.ferrotti@univpm.it (G. Ferrotti), f.canestrari@univpm.it (F. Canestrari).

1. Introduction

Nowadays, sustainability and circular economy are two main principles to be pursued in all industry sectors, including construction and building sectors (Ghisellini et al., 2016; Zavadskas et al., 2018). In the field of road pavement engineering, these two concepts can be put into practice in several ways, for instance through hot or cold recycling techniques, which, among the other benefits, allow the reuse of reclaimed asphalt pavement (RAP) from end-of-life pavements, thus reducing the need of new raw materials and avoiding the disposal of aged asphalt (Tam and Tam, 2006; Zaumanis et al., 2014). Another option is to increase the use of renewable materials, i.e., bio-materials not subjected to depletion, in order to reduce the dependence on non-renewable resources and hence the overall carbon footprint and greenhouse gas (GHG) emissions of the road industry (Fini et al., 2012; Ingrassia et al., 2019; Sun et al., 2016). Specifically, the general trend is to employ renewable materials that are residues and by-products of industrial activities or even of everyday life (Ingrassia et al., 2019; Yang et al., 2017). Indeed, further benefits can be achieved in this way, in terms of reduced need for landfills as well as disposal costs (Gong et al., 2016; Ingrassia et al., 2019; Yang et al., 2017).

Many types of renewable materials can be potentially employed for road application, provided that they possess a series of requirements in terms of availability, handling and logistics as well as non or limited impact on environment and workers' health (Ingrassia et al., 2019; Kluttz, 2012; Seidel and Haddock, 2012). In general, a broad distinction can be made between solid and liquid bio-materials (usually referred to as bio-oils), as it has been demonstrated that their addition to bituminous binders and mixtures provides different effects in terms of performance (Ingrassia et al., 2019). Examples of solid bio-materials are natural fibres (Oda et al., 2012) and lignin (Xu et al., 2017), while the liquid ones can be basically divided into four main groups (Ingrassia et al., 2019): wood bio-oils from paper and pulp industry (Bearsley and Haverkamp, 2007; Peralta et al., 2012; Yang et al., 2015), bio-oils from agricultural residues and vegetable biomass (Kowalski et al., 2016; Raouf and Williams, 2010; Seidel and Haddock, 2012), waste cooking oil (Gong et al., 2016; Sun et al., 2016; Wen et al., 2012), and bio-oils obtained from animal manure (Fini et al., 2012). Before the use of such bio-materials in bituminous binders and mixtures, however, a thermal and/or chemical pre-treatment is usually necessary (Ingrassia et al., 2019; Yang et al., 2017), such as fast pyrolysis (Peralta et al., 2012; Yang et al., 2015, 2017), esterification (Gong et al., 2016; Sun et al., 2016) or hydrothermal liquefaction (Fini et al., 2012).

The feasibility of very different bitumen replacement percentages has been investigated so far, employing renewable materials as modifiers (<10%) (Oda et al., 2012; Sun et al., 2016; Xu et al., 2017; Yang et al., 2017), extenders (25%—75%) (Wen et al., 2012; Yang et al., 2015) as well as direct alternative binders (100%) (Peralta et al., 2012; Raouf and Williams, 2010), depending on their characteristics (Ingrassia et al., 2019). Nevertheless, recent research has mainly focused on partial replacement of bitumen, approximately at percentages lower than 15%, and thus on the characterization of the resulting bio-binders, which can be defined as binders obtained by the blending of bitumen and a specific renewable material. In fact, the current limited scientific knowledge in terms of road application and the unpreparedness of the sector market make higher replacement percentages unlikely in the short or medium term (Ingrassia et al., 2019).

However, in order to make the use of bio-materials truly viable in road pavements, a comprehensive characterization of the resulting bio-binders is needed. In this perspective, this paper presents an extensive investigation of the chemical, morphological and rheological properties of bio-binders obtained by partially replacing bitumen with a wood bio-oil that is produced as a residue in the processing of wood into pulp and paper. Specifically, the chemical and morphological analyses aim at highlighting the basic chemical and structural modifications due to the bio-oil addition, while the objective of the rheological testing and modelling is to provide a performance-related characterization, which is useful to predict the actual mechanical behaviour of the bio-binders studied. In addition, the experimental investigation is completed by conventional and viscosity tests.

2. Materials and methods

2.1. Materials

A conventional 50/70 penetration grade bitumen was chosen as control bitumen in this experimental investigation. The wood bio-oil selected, whose characteristics are summarized in Table 1, was used in partial replacement of 50/70 bitumen according to different percentages by weight, with the aim

Table 1 — Characteristics of the bio-oil investigated.

Characteristic		Value
Kinematic viscosity (Comité Européen de Normalisation, 2015a)	at 60 °C	712 mm^2/s
	at 135 °C	26 mm^2/s
Elemental composition	Carbon	81.0%
	Hydrogen	11.0%
	Oxygen	7.5%

of identifying possible trends related to the bio-oil content in the characterization tests. Considering drastic substitution percentages of bitumen currently unrealistic (as anticipated in Section 1), 15% was chosen as a maximum feasible bio-oil percentage. Consequently, four binders were studied, as indicated in Table 2. The binders containing the bio-oil were prepared through a mixer, setting the blending speed at 500 rpm and the temperature at 150 °C for about 10 min.

2.2. Test procedures and experimental program

Fourier transform infrared spectroscopy (FTIR) was carried out to analyse the chemical composition of the pure bio-oil as well as the binders in terms of functional groups. The analysis was performed in reflection mode, with the attenuated total reflectance (ATR), by placing a drop of the material on the diamond crystal base plate of the spectrometer and measuring the absorbance at ambient temperature in a range of wavenumbers between 500 and 4000 cm^{-1}, with a resolution of 4 cm^{-1}. For each specimen, the spectrum resulting from the average of 32 scans was considered, and overall three specimens were tested for each material.

Thin layer chromatography with flame ionization detection (TLC-FID, commonly named Iatroscan) was performed according to Energy Institute (2006) in order to determine saturates, aromatics, resins and asphaltenes (SARA) fractions of the pure bio-oil and the binders. About 0.1 g of material was dissolved in dichloromethane to obtain a 2% solution, from which a small portion was applied to adsorption quartz rods filled with active silica (1 μL for each rod). Heptane, toluene-heptane (80:20) and dichloromethane-methanol (95:5) were then used in sequence on the rods to separate saturates, aromatics and resins respectively, leaving the asphaltenes not eluted. Five rods were analysed for each material.

In the microscopic analysis, a white light source was used to investigate the morphology of the binders in transmitted mode. Thin specimens were prepared by pouring a tiny drop of hot binder (heated at about 160 °C) on a glass plate, covered by a cover-glass, and then analysed at ambient temperature, considering a magnification between 100× and 400×.

Conventional properties, namely penetration and softening point, were determined according to Comité Européen de Normalisation (2015b, c).

The dynamic viscosity of the binders was determined using a Brookfield rotational viscometer according to ASTM (2015). Six temperatures were investigated: 80 °C, 90 °C, 105 °C, 120 °C, 135 °C and 150 °C. In order to evaluate the shear rate dependency of the binders, five measurements were performed at each temperature by considering

different working rates of the viscometer (10%, 30%, 50%, 70% and 90%), corresponding to different shear rates. For each binder, at least two specimens were tested.

The rheological properties of the binders were investigated through frequency sweep tests, carried out with a dynamic shear rheometer (DSR) in plate–plate configuration according to Comité Européen de Normalisation (2012). Nine temperatures were investigated, ranging from 0 °C to 80 °C with a step of 10 °C. At each testing temperature, the frequency was increased in logarithmic steps from 1 to 100 rad/s (i.e., from 0.159 to 15.9 Hz). All the tests were conducted at a low shear strain equal to 0.05%, which allowed all the specimens to be tested within the linear viscoelastic (LVE) domain. At least two specimens were tested for each binder.

2.3. 1S2P1D model

For thermo-rheologically simple materials such as conventional bitumens, the time–temperature superposition principle (TTSP) is valid and therefore the rheological results obtained in the LVE range for a limited interval of testing frequencies at different temperatures can be shifted in the frequency domain at a selected reference temperature. The modelling of the shifted experimental data allows to develop the master curves of the rheological properties, which are useful to predict the material behaviour in a significantly wider range of frequencies (and thus of temperatures) (Anderson et al., 1994).

In this study, a generalized version of the Huet-Sayegh rheological model (Sayegh, 1967), known as 2S2P1D (Olard and Di Benedetto, 2003), was considered for the modelling of the rheological results. The model consists of the combination of two springs, two parabolic elements and one dashpot, and was selected because of its general good adaptability to rheological experimental data. The expression of 2S2P1D model is as follows (Olard and Di Benedetto, 2003).

$$G^*(\omega) = G_0 + (G_g - G_0)/[1 + \alpha(i\omega\tau)^{-k} + (i\omega\tau)^{-h} + (i\omega\beta\tau)^{-1}] \qquad (1)$$

where the static modulus G_0 and the glassy modulus G_g represent the values of the complex modulus G^* when the frequency $\omega \to 0$ and when $\omega \to \infty$. respectively, and describe the behaviour of the springs, i is the complex number (defined as $i^2 = \sqrt{-1}$), k and h describe the behaviour of the parabolic elements, being $0 < k < h < 1$, α is a constant that represents the balance between the parabolic elements, the dashpot parameter β is related to the Newtonian viscosity of the model η, which is calculated according to Eq. (2).

$$\eta = (G_g - G_0)\beta\tau \qquad (2)$$

where τ is the characteristic time, which depends on temperature and accounts for TTSP and is defined by a shift factor law as in Eq. (3).

$$\tau = a_T(T)\tau_0 \qquad (3)$$

Table 2 – Binders studied.		
Binder code	50/70 bitumen (% by weight)	Bio-oil (% by weight)
50/70	100	0
50/70 + A5	95	5
50/70 + A10	90	10
50/70 + A15	85	15

where τ_0 is the value of τ at the selected reference temperature T_{ref}, and $a_T(T)$ is the shift factor at temperature T. For the temperatures typically investigated in the laboratory, a_T can be expressed by the Williams-Landel-Ferry (WLF) law in Eq. (4), where C_1 and C_2 are empirical constants.

$$\log(a_T) = -[C_1(T-T_{ref})]/[C_2 + (T-T_{ref})] \tag{4}$$

It can be observed from Eq. (1) that the rheological behaviour of the material is completely described through seven parameters (G_0, G_g, k, h, α, β, τ) (Olard and Di Benedetto, 2003; Perez-Martinez et al., 2016; Yusoff et al., 2013). However, considering also C_1 and C_2, nine parameters have to be determined in the modelling process overall.

When applying the 2S2P1D model to bituminous binders, the static modulus G_0 in Eq. (1) can be assumed equal to zero (Olard and Di Benedetto, 2003; Yusoff et al., 2013), thus the parameters to be determined become eight. In this case, since one spring can be removed, the model is usually named as 1S2P1D.

The same parameters can also be used to obtain the master curve of the phase angle δ through Eq. (5) after the storage modulus G_1 and the loss modulus G_2 have been determined (Yusoff et al., 2013).

$$\delta = \arctan(G_2/G_1) \tag{5}$$

In this experimental investigation, 20 °C was selected as the reference temperature for the master curves and the modelling was carried out by imposing the following conditions, which ensured a good fitting of the model to the experimental data. In Eq. (5), G_g was fixed equal to 10^9 Pa, as suggested in literature (Anderson et al., 1994), h was fixed equal to 0.56, while k was varied in a narrow range, between 0.22 and 0.25, in line with previous findings (Olard and Di Benedetto, 2003; Yusoff et al., 2013), α, β and τ_0 were varied without any restriction, as well as C_1 and C_2.

Specifically, the modelling procedure consisted in minimizing the error between the experimental data and the model.

3. Results and analysis

3.1. FTIR

The absorbance spectra obtained for one specimen of 50/70, 50/70 + A15 and pure bio-oil are presented in Fig. 1, from which it can be observed that the shape of the spectra is very similar from 2000 to 4000 cm^{-1} (Fig. 1(a)). Instead, in the range of wavenumbers between 500 and 2000 cm^{-1} (Fig. 1(b)), the spectra of the control bitumen and the pure bio-oil have different shapes but both exhibit peaks at 1700, 1600, 1460, 1376 and 1030 cm^{-1}, which correspond, respectively, to the C=O stretch of the carbonyl functional group, the C=C stretch of the aromatic group, the CH_2 and CH_3 bend of the aliphatic group and the S=O stretch of the sulfoxide group. Despite these similarities (which are due to the fact that both bitumen and bio-oil are composed of hydrocarbons), the bio-oil shows some additional peaks with respect to 50/70 bitumen. Specifically, a sharp peak at 1735 cm^{-1} and another peak around 1242 cm^{-1} can be noted, which are completely absent in the 50/70 bitumen spectrum. These peaks are due, respectively, to the C=O and C−O stretch of the esters and appear, to a lower extent, in the 50/70 + A15 spectrum as well (which however does not mean that a chemical reaction between bitumen and bio-oil has occurred). Therefore, these two peaks can be reasonably considered as a useful means for quantifying the content of the bio-oil investigated.

In order to compare the materials tested in detail, the spectral analysis was carried out through an integration method consisting in determining the area below the absorbance spectrum around the abovementioned peaks.
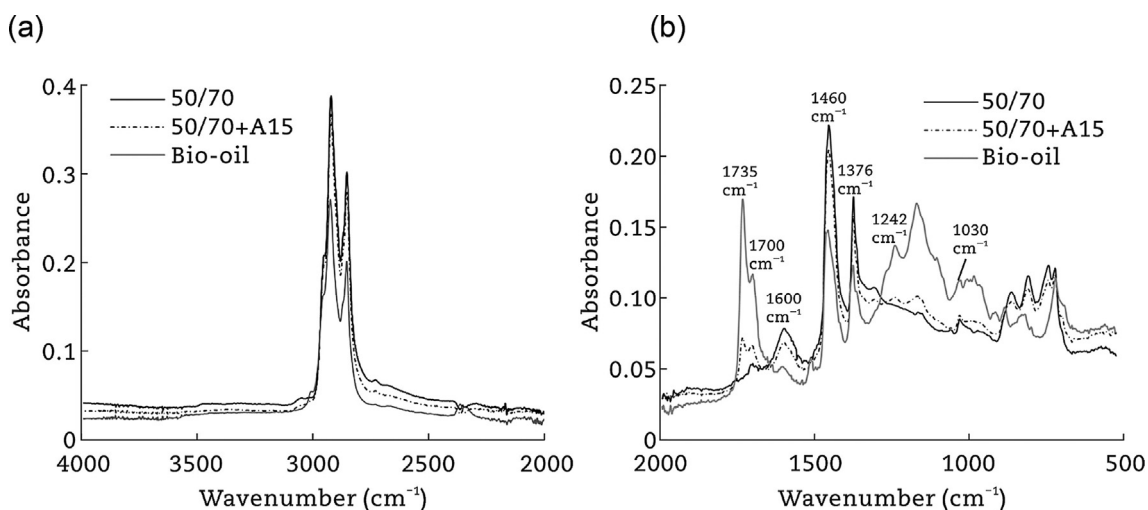

Fig. 1 − FTIR spectra of 50/70, 50/70 + A15 and pure bio-oil. (a) From 2000 to 4000 cm^{-1}. (b) From 500 to 2000 cm^{-1}.

Specifically, a tangential approach was considered, namely a relative base line tangential to the spectrum was chosen for each peak (Hofko et al., 2017, 2018). Consequently, seven areas were determined for each specimen and then the average and standard deviation were calculated for each material, as summarized in Table 3.

The results clearly confirm that the ester areas A_{1735} and A_{1242} can be effectively considered to detect the presence of the bio-oil studied in bituminous binders. Indeed, their values, which are equal to zero for 50/70 bitumen, progressively increase along with the amount of the bio-material. The aliphatic absorbance of the binder seems to be slightly reduced by the addition of the bio-oil, probably because the latter is characterized by lower A_{1460} and A_{1376} compared to the control bitumen. A similar observation can be made for the sulfoxide area, even though it should be highlighted that the addition of the bio-material alters the shape of the spectrum for wavenumbers approximately between 920 and 1050 cm^{-1}, making the peak at 1030 cm^{-1} less distinct (Fig. 1(b)). Therefore, the sulfoxide index might not be suitable for studying the aging of such bio-binders, unlike conventional bitumens. Moreover, an evident reduction, which is greater with increasing content of bio-oil, occurs for A_{1600}, as the aromatic peak at 1600 cm^{-1} is much less prominent in the bio-oil spectrum compared to the 50/70 one (Fig. 1(b)). On the contrary, the carbonyl area at 1700 cm^{-1} has a general trend to increase with the amount of bio-oil, but in this case the differences between the binders have the same order of magnitude as the standard deviation, thus not allowing a firm conclusion to be drawn. However, this increment seems reasonable considering that the pure bio-material is characterized by a greater value of A_{1700} with respect to the control bitumen.

3.2.   SARA fractions

A qualitative comparison of the chromatograms obtained for one rod of the control bitumen and one rod of the pure bio-oil is shown in Fig. 2(a). The difference between the chromatograms is very evident, as 50/70 presents — as expected — four peaks corresponding to saturates, aromatics, resins and asphaltenes, whereas the bio-material exhibits only the peaks of (by definition) aromatics and resins plus a very small one for asphaltenes, while saturates are completely absent. Moreover, it should be noted that, for the bio-oil, the retention times of aromatics and resins are rather different from those of the control bitumen. The higher retention times observed could be due to a stronger affinity with the stationary phase, determined by the high polarity of the bio-oil. For the bio-binders, this difference in the retention resulted in an additional peak between aromatics and resins (Fig. 2(b)), which was included in the

Table 3 — FTIR peak areas.										
Peak area	Absorption mode	50/70		50/70 + A5		50/70 + A10		50/70 + A15		Bio-oil	
		Average	Std. dev.	Average	Std. dev.	Average	Std. dev.	Average	Std. dev.	Average	Std. dev.
A_{1700}	C=O stretch	0.126	0.003	0.122	0.024	0.138	0.009	0.143	0.013	0.371	0.020
A_{1600}	C=C stretch	1.512	0.003	1.380	0.039	1.197	0.041	0.989	0.033	0.180	0.003
A_{1460}	CH$_2$ bend	5.709	0.003	5.535	0.062	5.414	0.111	5.059	0.066	3.553	0.037
A_{1376}	CH$_3$ bend	1.551	0.008	1.561	0.012	1.545	0.018	1.467	0.004	1.328	0.021
A_{1030}	S=O stretch	0.256	0.013	0.202	0.017	0.132	0.004	0.118	0.007	0.136	0.012
A_{1735}	C=O stretch	0.000	0.000	0.111	0.002	0.240	0.023	0.334	0.008	1.723	0.045
A_{1242}	C—O stretch	0.000	0.000	0.049	0.004	0.100	0.008	0.164	0.007	0.858	0.009

Note: Std. dev. means standard deviation.
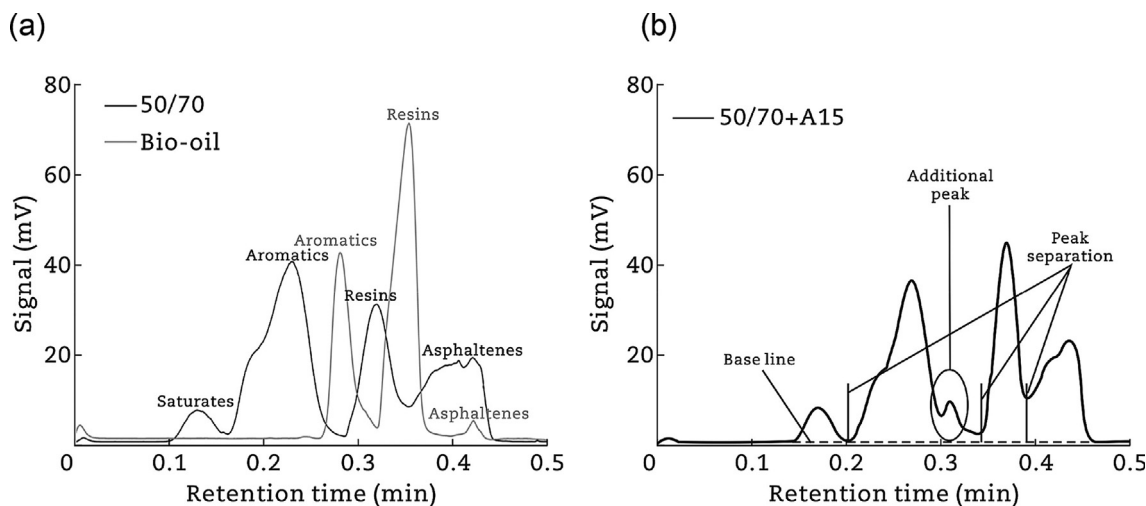
Fig. 2 — Comparison of chromatograms. (a) 50/70 and pure bio-oil. (b) 50/70 + A15.

Material	Saturates (%)	Aromatics (%)	Resins (%)	Asphaltenes (%)	Resins + asphaltenes (%)	Colloidal index
50/70	5.7	47.3	21.8	25.2	47.0	0.45
50/70 + A5	5.4 (5.4)	46.5 (46.6)	24.4 (23.9)	23.9 (24.1)	48.3 (48.0)	0.41 (0.42)
50/70 + A10	4.9 (5.1)	45.5 (45.9)	24.6 (26.1)	25.0 (22.9)	49.6 (49.0)	0.43 (0.39)
50/70 + A15	4.9 (4.8)	44.8 (45.2)	27.2 (28.2)	23.1 (21.8)	50.3 (50.0)	0.39 (0.36)
Bio-oil	0.0	33.2	64.3	2.5	66.8	0.03

Table 4 – SARA fractions: experimental and estimated (in brackets) values.

aromatics in the quantitative analysis performed later. On the contrary, no additional peak emerged between resins and asphaltenes (Fig. 2(b)), but in some cases an imperfect separation between such peaks was observed. For this reason, the sum of these two fractions was also considered.

In order to quantify the SARA fractions, the chromatogram related to each rod was integrated by considering a common base line for all peaks and separating the fractions as shown in Fig. 2(b), thus determining the area of every peak. Afterwards, for every single rod, the relative percentage of each fraction was calculated by dividing the corresponding peak area by the total area. The values presented in Table 4 were then obtained by averaging the results of the rods analysed for each material. Furthermore, based on the results achieved for 50/70 and the pure bio-oil and assuming no chemical reaction between them after blending, the values of SARA fractions for the bio-binders were also estimated through a simple mathematical calculation and shown in Table 4 in brackets, for comparison with the experimental values. The estimation was made considering Eq. (6), given for the resins for simplicity but valid for all fractions.

$$\text{est.resins}_{50/70+Ax} = [(100-x)/100]\exp.\text{resins}_{50/70}+(x/100)\exp.\text{resins}_{\text{bio-oil}} \tag{6}$$

where x is the bio-oil amount (5%, 10% or 15%), "est.resins" and "exp.resins" indicate the estimated and experimental value, respectively.

From the experimental results summarized in Table 4, it can be noted that a trend linked with the bio-oil content exists for all fractions. Specifically, as the amount of bio-oil increases, saturates, aromatics and asphaltenes are progressively reduced, while resins are markedly increased. The only exception is represented by 50/70 + A10, for which the resins' content seems slightly underestimated while the asphaltenes' amount slightly overestimated due to a poor separation between the two fractions (their sum is in fact in line with the other results). In general, the small differences observed from the comparison of the experimental and estimated values (Table 4) also suggest that only a physical blending seems to occur between bitumen and bio-oil, without any chemical reaction.

Moreover, from the experimental data, the colloidal index (CI) was easily calculated according to Eq. (7), in order to predict the effect provided by the bio-oil addition in terms of conventional properties (Mangiafico et al., 2016).

$$\text{CI}=(\text{asphaltenes} + \text{saturates})/(\text{aromatics} + \text{resins}) \tag{7}$$

Based on literature (Mangiafico et al., 2016), it is expected that the reduction of asphaltenes and CI caused by the bio-oil (Table 4) leads to an increase of penetration and a decrease of the softening point. It is worth pointing out that, for 50/70 + A10, the value of CI is affected by the partial overlapping of resins and asphaltenes.

In addition, it can be assumed that the reduced aromaticity, detected also from FTIR analysis (Table 3), might affect the viscoelastic properties of the binders (Soenen and Redelius, 2014).

3.3. Morphology

Fig. 3 shows the images obtained from the microscopic analysis for the control bitumen, 50/70, and the bio-binder with the maximum amount of bio-oil studied, i.e., 15%, with a magnification equal to 200×. It is evident that 50/70 + A15 presents a perfectly homogeneous structure without any phase separation, which is exactly like the control bitumen. The images referring to lower bio-oil contents (5% and 10%) and different magnifications are not shown here, as they look very similar to the ones provided.

This outcome confirms that little energy is required for blending bitumen and the selected bio-material and also suggests that no problems in terms of storage stability should emerge for the binders investigated.

3.4. Conventional properties

The results of the conventional tests are summarized in Table 5, which shows that the bio-material provides a consistency reduction that results in increased penetration and decreased softening point, and the effect is higher as its dosage increases, in accordance with the outcomes of SARA analysis.

The results of the tests were also used to calculate the penetration index (PI) in order to estimate the temperature susceptibility of the binders at intermediate temperatures (Hunter et al., 2015)

$$\text{PI} = [1952-500\log(\text{Pen}_{25})-20\text{SP}]/[50\log(\text{Pen}_{25})-\text{SP}-120] \tag{8}$$

where Pen_{25} is the penetration at 25 °C (0.1 mm) and SP is the softening point (°C). Specifically, the temperature susceptibility is higher when PI is lower. The results obtained suggest that the addition of the bio-oil has a small influence on the temperature susceptibility, as the variation of PI is limited (Table 5).
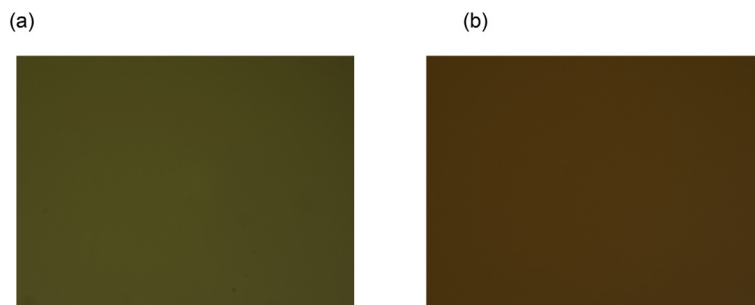
Fig. 3 — Images obtained from the microscopic analysis (with 200× magnification). (a) 50/70. (b) 50/70 + A15.

Moreover, based on penetration, softening point and PI, the potential penetration grade class of the bio-binders was predicted according to the specifications required by Comité Européen de Normalisation (2009). As can be seen from Table 5, each increase of 5% bio-oil leads to a softer grade class. However, it is worth pointing out that, for a thorough classification of the bio-binders, more tests are necessary, especially including the evaluation of aging.

3.5. Viscosity

The results of the viscosity tests are shown in Fig. 4. Six series of points are plotted for each binder, corresponding to the temperatures investigated. Specifically, for each binder, the highest viscosity value corresponds to the lowest testing temperature (80 °C), while the lowest viscosity value corresponds to the highest testing temperature (150 °C). In general, lower shear rates were imposed at lower temperatures, because the higher viscosity of the binder implies a higher working rate of the viscometer and thus smaller shear rates have to be considered.

From the results obtained, a Newtonian behaviour can be assumed for all binders at all testing temperatures, as the viscosity is almost independent of the shear rate. Note that at the highest temperature (150 °C), some experimental points are missing, since shear rates higher than 200 s^{-1} cannot be investigated with the equipment employed.

Since the assumption of Newtonian behaviour is valid, the viscosity value measured at a working rate of the viscometer equal to 50% was considered in order to further compare the binders (Fig. 5(a)). A progressive viscosity reduction is obtained as the dosage of bio-oil increases, being the control bitumen the most viscous binder and 50/70 + A15 the least

viscous binder at all testing temperatures. However, a significant decrease in viscosity is observed after the addition of 5% bio-oil, whereas the decrease is less evident when its amount is further increased, as can be seen from the values of Δ, which represents the viscosity percentage reduction with respect to 50/70 bitumen, calculated according to Eq. (9) and provided in Fig. 5(b).

$$\Delta_i\ (\%) = 100[(\eta_{50/70}-\eta_i)/\eta_{50/70}] \qquad (9)$$

where η is the dynamic viscosity, and i is 50/70 + A5, 50/70 + A10, or 50/70 + A15.

Based on these results, the bio-oil examined, which is able to considerably reduce bitumen viscosity even in small quantities, might also be employed to promote the self-healing of bituminous mixtures. Indeed, according to a technique recently developed (Garcia et al., 2010; Norambuena-Contreras et al., 2018), low-viscosity oils can be encapsulated and incorporated in the mixture. Then, the formation of cracks will break the capsule shell, allowing the oil to be released. In this way, the oil will reduce the viscosity of bitumen, which will be able to flow into the cracks, providing self-healing.

Considering the reference Superpave viscosity values for mixing and compacting bituminous mixtures (0.17 Pa·s and 0.28 Pa·s, respectively) (Kennedy et al., 1994), the potential mixing and compaction temperatures for the binders were determined through the regression of the experimental data on the log(logη)-temperature diagram. From Table 6, it can be observed that the working temperatures can be reduced up to 10 °C with respect to 50/70 bitumen when the dosage of the bio-material is equal to or lower than 10%, while a potential reduction of about 15 °C can be achieved with 15% dosage. This reduction was somehow expected because of

Table 5 — Penetration, softening point and penetration index values with consequent potential penetration grade class.

Binder	Penetration (0.1 mm)	Softening point (°C)	Penetration index	Potential penetration grade class
50/70	51.5	49.7	−1.21	—
50/70 + A5	71.3	47.0	−1.16	70/100
50/70 + A10	114.4	43.5	−0.87	100/150
50/70 + A15	153.5	39.8	−1.25	160/220

Fig. 4 — Dynamic viscosity as a function of shear rate.

susceptibility. Results show that there is not a clear correlation between VTS value and bio-oil dosage, confirming what has been previously observed in terms of penetration index and thus allowing to conclude that the bio-material studied does not significantly affect the temperature susceptibility of bituminous binders.

3.6. Rheology

The raw rheological results obtained from the frequency sweep tests are plotted in Fig. 6(a) and (b), which show, respectively, the Black diagram and the Cole–Cole diagram.

From Fig. 6(a), it can be observed that all binders tested exhibit a thermo-rheologically simple behaviour, as the experimental data obtained at different temperatures and frequencies align along the same curve, thus allowing the master curves of the rheological properties to be obtained (Airey, 2002). The binders begin to lose their thermo-rheological simplicity at high temperatures, i.e., when the phase angle approaches 90°. This is true particularly for 50/70 + A15, as some experimental points are evidently not aligned with the others, suggesting that bio-binders with bio-oil dosages higher than 15% might only have a partial thermo-rheologically simple behaviour.

As for the comparison between the binders, the increasing amount of bio-oil causes a progressive shift of the experimental data towards right and down in the Black diagram (i.e., higher values of phase angle δ and lower values of complex modulus $|G^*|$ as in Fig. 6(a)), and towards left and down in the Cole–Cole diagram (i.e., lower storage modulus G_1 and loss modulus G_2 as in Fig. 6(b)). Nevertheless, the differences between the binders are not very apparent from the Black and Cole–Cole diagrams.

A further comparison between the binders in terms of rheological behaviour is provided in Fig. 7, which shows the master curves of complex modulus and phase angle at 20 °C, as well as in Fig. 8, which presents the master curves of storage modulus and loss modulus at 20 °C. The 1S2P1D and WLF parameters deriving from the modelling are summarized in Table 8.

Firstly, it should be noted the 1S2P1D model fits quite well the experimental data in terms of complex modulus as well as storage and loss moduli, for all binders. Some imprecision can
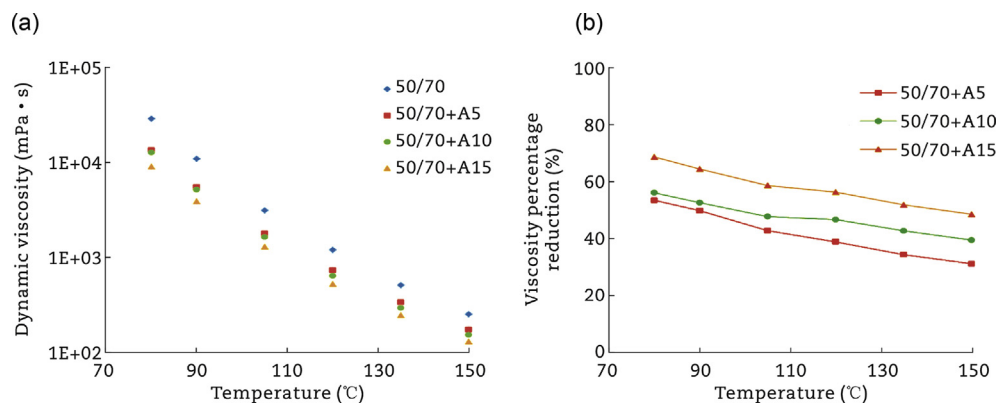
the softening effect provided by the bio-oil and such working temperatures should be compared to those of conventional bitumens having analogous penetration.

In order to assess the temperature susceptibility of the binders at high temperatures, the regression of the viscosity-temperature relationship was considered, according to Eq. (10) (ASTM, 2016; Cardone et al., 2014).

$$\log(\log \eta) = \text{RI} + \text{VTS}\log T \qquad (10)$$

where η is the viscosity (mPa·s), RI is the regression intercept, VTS is the regression slope that represents the viscosity-temperature susceptibility parameter, and T is the temperature (°R). The results of the regression are given in Table 7, together with the coefficient of determination R^2, whose values (very close to 1) demonstrate that Eq. (10) characterizes the viscosity-temperature relationship very well for the bio-binders studied. In general, a lower absolute value of VTS indicates a less pronounced temperature

Fig. 5 — Analysis of viscosity data. (a) Dynamic viscosity as a function of temperature. (b) Viscosity percentage reduction with respect to 50/70 bitumen.

Table 6 — Potential mixing and compaction temperatures for the binders tested.

Binder	Mixing temperature (°C)	Compaction temperature (°C)
50/70	159	148
50/70 + A5	149	138
50/70 + A10	147	137
50/70 + A15	143	133

Table 7 — Regression parameters of the viscosity-temperature relationship.

Binder	RI	VTS	R^2
50/70	10.239	−3.4214	0.9998
50/70 + A5	10.073	−3.3741	0.9999
50/70 + A10	10.412	−3.4960	0.9999
50/70 + A15	10.336	−3.4743	1.0000

be observed only at low reduced frequency (i.e., high temperatures). Moreover, the effect of the reduced thermo-rheological simplicity previously highlighted mainly emerges in the storage modulus master curve at low frequencies for high dosages of bio-oil ($\geq$10%), as the experimental data are not perfectly aligned (Fig. 8(a)). In terms of phase angle, instead, the model fitting is less accurate (especially at intermediate frequencies), but the ranking of the different binders is respected (Fig. 7(b)). The slight inaccuracy in the modelling

of the phase angle has been already highlighted in literature (Olard and Di Benedetto, 2003; Yusoff et al., 2013).

Fig. 7 confirms what previously observed from the Black diagram, namely the bio-material produces a reduction of complex modulus $|G^*|$ and an increase of phase angle δ, which are more pronounced for higher dosages. These effects emerge in a wide range of reduced frequencies, indicating that an improvement of the low-temperature performance of the binder might be achieved thanks to the decreased stiffness and elasticity provided by the addition of the bio-oil, whereas, on the other hand, the high-temperature behaviour might be negatively affected. Moreover, Fig. 8 suggests that the reduction of $|G^*|$ is predominant with respect to the increase of δ, since both G_1 and G_2 are progressively reduced with increasing bio-oil content.

In terms of 1S2P1D parameters (Table 8), β seems to remain about constant, regardless of the bio-material dosage. Conversely, a significant reduction of α and τ_0 is observed as the bio-oil amount increases, due to its softening effect. This result is in agreement with literature, as softer binders are typically characterized by lower values of α, β and/or τ_0 (Olard and Di Benedetto, 2003; Perez-Martinez et al., 2016; Yusoff et al., 2013). Moreover, for binders ($G_0 = 0$), at very high temperatures (or analogously very low frequencies), the rheological model is equivalent to a linear dashpot (Olard and Di Benedetto, 2003) whose behaviour is governed by Eq. (2). Being in this case G_g and β constant, the reduction of τ
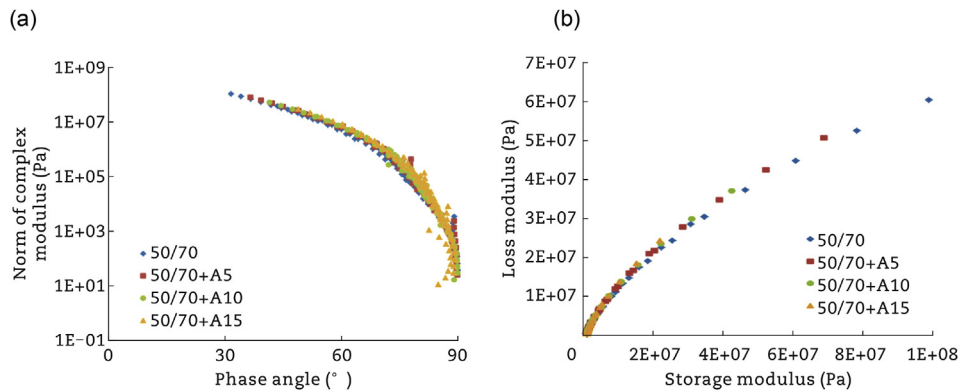

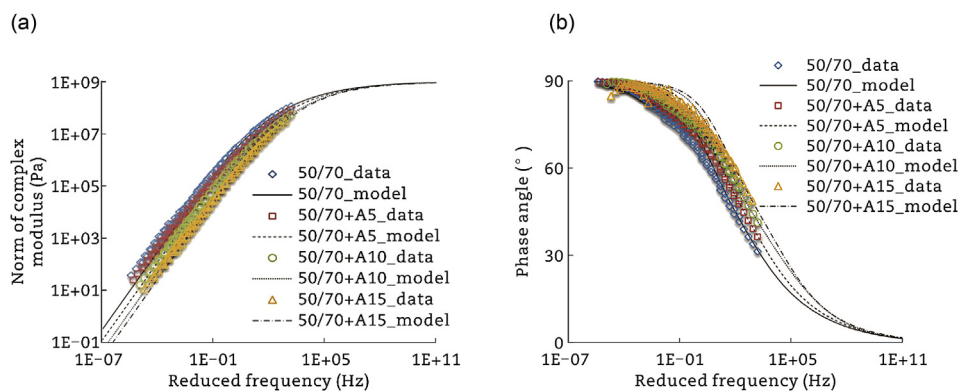Fig. 6 — Raw rheological results. (a) Black diagram. (b) Cole—Cole diagram.

Fig. 7 — Master curves (at a reference temperature of 20 °C). (a) Complex modulus. (b) Phase angle.
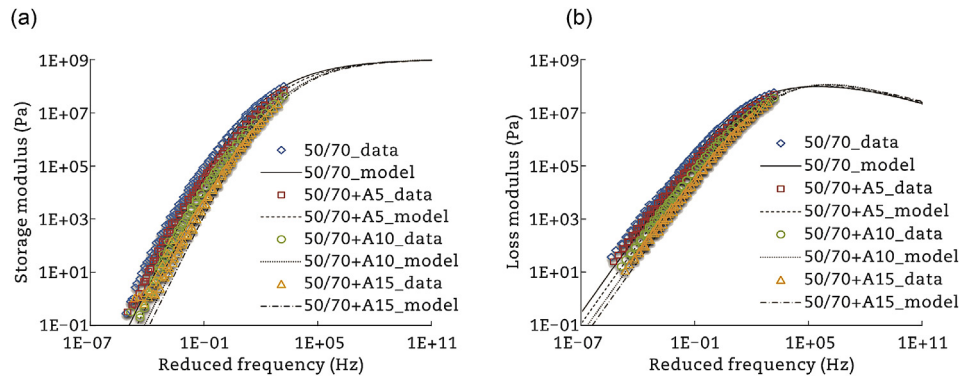
Fig. 8 − Master curves (at a reference temperature of 20 °C). (a) Storage modulus. (b) Loss modulus.

Table 8 − 1S2P1D and WLF parameters.

Binder	G_g (Pa)	k	h	α	$\log \beta$	$\log \tau_0$	C_1	C_2
50/70	1.00E+09	0.22	0.56	2.4	1.74	−5.05	25	262
50/70 + A5	1.00E+09	0.22	0.56	2.2	1.73	−5.44	23	248
50/70 + A10	1.00E+09	0.25	0.56	2.0	1.74	−5.85	17	188
50/70 + A15	1.00E+09	0.22	0.56	1.7	1.73	−6.10	23	286

generates a decrease of the Newtonian viscosity of the model η (Eq. (2)) that seems to be consistent with the viscosity reduction observed from the experiments at high temperatures (Fig. 5).

As for the WLF parameters (Table 8), C_1 and C_2 seem to decrease as the bio-oil dosage increases, even though 50/70 + A15 does not follow this trend. The reduction of C_1 and C_2 might also be a consequence of the softening effect provided by the bio-material.

3.7. Rutting and fatigue tendency

In order to provide a more effective performance-based characterization, an indication of the rutting and fatigue tendency of the binders studied was obtained by calculating the Superpave parameters (Kennedy et al., 1994) from the rheological data available. The results are shown in Fig. 9, where the small error bars represent the standard deviation.

The rutting parameter $|G^*|/\sin \delta$ was determined at 10 rad/s (i.e., 1.59 Hz) at four temperatures: 50 °C, 60 °C, 70 °C, 80 °C (Fig. 9(a)). The higher is the value of $|G^*|/\sin \delta$, the higher is the resistance of the binder to permanent deformation, and thus the lower the rutting tendency of the resulting mixture should be (Kennedy et al., 1994). A value of 1 kPa is assumed as a reference in unaged condition, the situation in which the binder is usually more deformable. As can be seen from Fig. 9(a), the increasing addition of bio-oil causes a progressive reduction of $|G^*|/\sin \delta$ and therefore a worsening of the resistance to permanent deformation and rutting at high service temperatures. Specifically, for 50/70 + A15, $|G^*|/\sin \delta$ is lower than 1 kPa at 60 °C, while for 50/70 + A5 and 50/70 + A10, the requirement is no longer met at 70 °C. On the contrary, the control bitumen still shows a value greater than 1 kPa at 70 °C. The results indicate that the upper performance grade (PG) limit, the temperature at which no problems in terms of rutting occur, might be between 50 °C and 60 °C for 50/70 + A15, between 60 °C and 70 °C for 50/70 + A5 and 50/70 + A10, and between 70 °C and 80 °C for the control bitumen.

Nevertheless, it should be pointed out that the bio-binders differ from the studied base bitumen in terms of penetration grade. A more reasonable comparison probably should be made by considering bitumens with similar penetrations to those of the bio-binders. Moreover, since this effect has already been detected in previous research concerning bio-
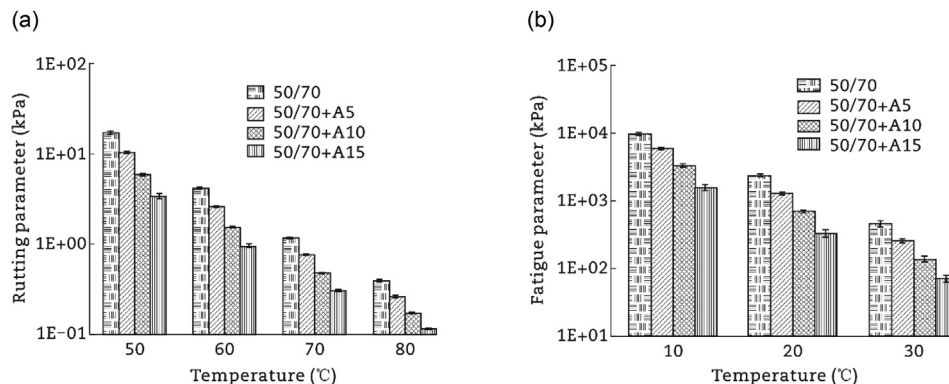

Fig. 9 − Superpave parameters. (a) Rutting. (b) Fatigue.

oils (Sun et al., 2016; Zhang et al., 2017a), several solutions have been proposed in literature to improve the high-temperature performance of bio-binders, such as the addition of crumb rubber (Peralta et al., 2012), polymers (Zhang et al., 2017b) and bio-polymers (e.g., lignin) (Kowalski et al., 2016; Xu et al., 2017), which have the potential to extend the range of applicability temperatures of the binders.

The fatigue parameter |G*|sin δ was calculated at 10 rad/s (1.59 Hz) at three intermediate service temperatures: 10 °C, 20 °C, and 30 °C (Fig. 9(b)). In this case, lower values of the parameter indicate a better resistance of the binder to fatigue cracking (Kennedy et al., 1994). The evaluation of |G*|sin δ is normally required after long-term aging, as the binder is stiffer and thus more prone to cracking. Therefore, the results presented, which refer to unaged binders, only give an indication of the possible effect of the bio-oil on the fatigue resistance. Fig. 9(b) shows that the bio-material provides a reduction of |G*|sin δ and this effect is more apparent as its dosage increases, suggesting that an improvement of the fatigue resistance might be achieved. Also in this case, the observed fatigue behaviour of the bio-binders should be compared to that of bitumens with equal penetration.

4.   Conclusions

The objective of this study is to provide an extensive characterization of the properties of bio-binders obtained by partially replacing a conventional 50/70 bitumen with a wood bio-oil at four different percentages: 0, 5%, 10% and 15%. Various tests were performed, including chemical, morphological and rheological as well as conventional and viscosity tests. Rheological modelling was also carried out. Based on the results and analyses presented, the following conclusions can be drawn.

- In terms of functional groups, the main effects provided by the addition of bio-oil to bitumen are the development of new peaks related to esters and a significant reduction of aromatics.
- In terms of SARA fractions, the bio-binders present reduced saturates, aromatics and asphaltenes along with increased resins compared to the control bitumen.
- When mixed together, the bitumen and the wood bio-oil seem to undergo only a physical blending, without any chemical reaction.
- The microscopic investigation demonstrates that the bio-binders are completely homogeneous, and therefore no concerns in terms of blending energy and storage stability are expected.
- The bio-material provides a consistency reduction, namely penetration increases while softening point decreases, producing binders with a softer grade.
- A Newtonian behaviour can be assumed for all the binders tested and, as the dosage of the bio-material increases, a progressive viscosity reduction is observed.
- Temperature susceptibility does not seem to be significantly affected by the bio-material.

- A thermo-rheologically simple behaviour is observed up to 15% of the bio-material. The bio-oil causes an increase in the phase angle and a reduction of the complex modulus, which seems to be predominant in a wide range of frequencies.
- Overall, a good fitting of the rheological data can be achieved with 1S2P1D model, especially in terms of complex modulus. Moreover, the decrease of the parameter τ_0, which is more evident as the bio-oil dosage increases, seems to be reasonably consistent with the viscosity reduction observed.

These findings indicate that overall the wood bio-oil examined is suitable to be used in partial replacement of bitumen for road applications. Its addition provides, in terms of performance, a softening effect that could be favourably exploited for instance to produce binders, able to resist to thermal and fatigue cracking in cold climates, reduce the mixing and compaction temperatures of bituminous mixtures without affecting their workability, or rejuvenate aged bitumen from reclaimed asphalt in recycling operations. Another potential application might be to produce capsules containing bio-oil and incorporate them in the bituminous mixture, with the aim of promoting self-healing when cracking occurs.

Future work will be aimed at investigating the aging properties of such bio-binders, assessing the adhesion with aggregate and evaluating recyclability aspects.

Conflict of interest

The authors do not have any conflict of interest with other entities or researchers.

R E F E R E N C E S

Airey, G.D., 2002. Use of Black diagrams to identify inconsistencies in rheological data. Road Materials and Pavement Design 3 (4), 403–424.

Anderson, D.A., Christensen, D.W., Bahia, H.U., et al., 1994. Binder Characterization and Evaluation, Volume 3: Physical Characterization. SHRP Report A-369. National Research Council, Washington DC.

ASTM, 2016. Standard Practice for Viscosity-Temperature Chart for Asphalt Binders. D2493. ASTM, West Conshohocken.

ASTM, 2015. Standard Test Method for Viscosity Determination of Asphalt at Elevated Temperatures Using a Rotational Viscometer. D4402. ASTM, West Conshohocken.

Bearsley, S.R., Haverkamp, R.G., 2007. Age hardening potential of tall oil pitch modified bitumen. Road Materials and Pavement Design 8 (3), 467–481.

Cardone, F., Ferrotti, G., Frigio, F., et al., 2014. Influence of polymer modification on asphalt binder dynamic and steady flow viscosities. Construction and Building Materials 71, 435–443.

Comité Européen de Normalisation (CEN), 2009. Bitumen and Bituminous Binders – Specifications for Paving Grade Bitumens. 12591. CEN, Brussels.

Comité Européen de Normalisation (CEN), 2015a. Bitumen and Bituminous Binders – Determination of Kinematic Viscosity. 12595. CEN, Brussels.

J. Traffic Transp. Eng. (Engl. Ed.) 2020; 7 (2): 192—204

203

Comité Européen de Normalisation (CEN), 2015b. Bitumen and Bituminous Binders − Determination of Needle Penetration. 1426. CEN, Brussels.

Comité Européen de Normalisation (CEN), 2015c. Bitumen and Bituminous Binders − Determination of the Softening Point − Ring and Ball Method. 1427. CEN, Brussels.

Comité Européen de Normalisation (CEN), 2012. Bitumen and Bituminous Binders − Determination of Complex Shear Modulus and Phase Angle − Dynamic Shear Rheometer (DSR). 14770. CEN, Brussels.

Energy Institute, 2006. Determination of Saturated, Aromatic and Polar Compounds in Petroleum Products by Thin Layer Chromatography and Flame Ionization Detection. IP 469. Energy Institute, London.

Fini, E.H., Al-Qadi, I.L., You, Z., et al., 2012. Partial replacement of asphalt binder with bio-binder: characterisation and modification. International Journal of Pavement Engineering 13 (6), 515—522.

Garcia, A., Schlangen, E., van de Ven, M., et al., 2010. Preparation of capsules containing rejuvenators for their use in asphalt concrete. Journal of Hazardous Materials 184 (1−3), 603—611.

Ghisellini, P., Cialani, C., Ulgiati, S., 2016. A review on circular economy: the expected transition to a balanced interplay of environmental and economic systems. Journal of Cleaner Production 114, 11—32.

Gong, M., Yang, J., Zhang, J., et al., 2016. Physical-chemical properties of aged asphalt rejuvenated by bio-oil derived from biodiesel residue. Construction and Building Materials 105, 35—45.

Hofko, B., Alavi, M.Z., Grothe, H., et al., 2017. Repeatability and sensitivity of FTIR ATR spectral analysis methods for bituminous binders. Materials and Structures 50 (3), 187.

Hofko, B., Porot, L., Cannone, A.F., et al., 2018. FTIR spectral analysis of bituminous binders: reproducibility and impact of ageing temperature. Materials and Structures 51 (2), 45.

Hunter, R.N., Self, A., Read, J., 2015. The Shell Bitumen Handbook, sixth ed. Thomas Telford Ltd., London.

Ingrassia, L.P., Lu, X., Ferrotti, G., et al., 2019. Renewable materials in bituminous binders and mixtures: speculative pretext or reliable opportunity? Resources, Conservation and Recycling 144, 209—222.

Kennedy, T.W., Huber, G.A., Harrigan, E.T., et al., 1994. Superior Performing Asphalt Pavements (Superpave): the Product of the SHRP Asphalt Research Program. SHRP Report A-410. National Research Council, Washington DC.

Kluttz, R., 2012. Considerations for use of alternative binders in asphalt pavements − material characteristics. Transportation Research Circular E- C165, 2—6.

Kowalski, K.J., Król, J., Radziszewski, P., et al., 2016. Eco-friendly materials for a new concept of asphalt pavement. Transportation Research Procedia 14, 3582—3591.

Mangiafico, S., Di Benedetto, H., Sauzéat, C., et al., 2016. Effect of colloidal structure of bituminous binder blends on linear viscoelastic behaviour of mixtures containing reclaimed asphalt pavement. Materials and Design 111, 126—139.

Norambuena-Contreras, J., Yalcin, E., Garcia, A., et al., 2018. Effect of mixing and ageing on the mechanical and self-healing properties of asphalt mixtures containing polymeric capsules. Construction and Building Materials 175, 254—266.

Oda, S., Fernandes Jr., J.L., Ildefonso, J.S., 2012. Analysis of use of natural fibers and asphalt rubber binder in discontinuous asphalt mixtures. Construction and Building Materials 26 (1), 13—20.

Olard, F., Di Benedetto, H., 2003. General "2S2P1D" model and relation between the linear viscoelastic behaviours of bituminous binders and mixes. Road Materials and Pavement Design 4 (2), 185—224.

Peralta, J., Williams, R.C., Rover, M., et al., 2012. Development of rubber-modified fractionated bio-oil for use as noncrude petroleum binder in flexible pavements. Transportation Research Circular E-C165, 23—36.

Perez-Martinez, M., Marsac, P., Gabet, T., et al., 2016. Prediction of the mechanical properties of aged asphalt mixes from FTIR measurements. In: 8th RILEM International Symposium on Testing and Characterization of Sustainable and Innovative Bituminous Materials, Ancona, 2016.

Raouf, M.A., Williams, C.R., 2010. General rheological properties of fractionated switchgrass bio-oil as a pavement material. Road Materials and Pavement Design 11, 325—353.

Sayegh, G., 1967. Viscoelastic properties of bituminous mixtures. In: The Second International Conference on Structural Design of Asphalt Pavement, Ann Arbor, 1967.

Seidel, J.C., Haddock, J.E., 2012. Soy fatty acids as sustainable modifier for asphalt binders. Transportation Research Circular E-C165, 15—22.

Soenen, H., Redelius, P., 2014. The effect of aromatic interactions on the elasticity of bituminous binders. Rheological Acta 53 (9), 741—754.

Sun, Z., Yi, J., Huang, Y., et al., 2016. Properties of asphalt binder modified by bio-oil derived from waste cooking oil. Construction and Building Materials 102, 496—504.

Tam, V.W.Y., Tam, C.M., 2006. A review on the viable technology for construction waste recycling. Resources, Conservation and Recycling 47 (3), 209—221.

Wen, H., Bhusal, S., Wen, B., 2012. Laboratory evaluation of waste cooking oil-based bioasphalt as a sustainable binder for hot-mix asphalt. Journal of Materials in Civil Engineering 25 (10), 1432—1437.

Xu, G., Wang, H., Zhu, H., 2017. Rheological properties and anti-aging performance of asphalt binder modified with wood lignin. Construction and Building Materials 151, 801—808.

Yang, X., Mills-Beale, J., You, Z., 2017. Chemical characterization and oxidative aging of bio-asphalt and its compatibility with petroleum asphalt. Journal of Cleaner Production 142, 1837—1847.

Yang, X., You, Z., Mills-Beale, J., 2015. Asphalt binders blended with a high percentage of biobinders: aging mechanism using FTIR and rheology. Journal of Materials in Civil Engineering 27 (4), 04014157.

Yusoff, N.I.M., Mounier, D., Marc-Stéphane, G., et al., 2013. Modelling the rheological properties of bituminous binders using the 2S2P1D model. Construction and Building Materials 38, 395—406.

Zaumanis, M., Mallick, R.B., Frank, R., 2014. 100% recycled hot mix asphalt: a review and analysis. Resources, Conservation and Recycling 92, 230—245.

Zavadskas, E.K., Antucheviciene, J., Vilutiene, T., et al., 2018. Sustainable decision-making in civil engineering, construction and building technology. Sustainability 10 (1), 1—21.

Zhang, L., Bahia, H., Tan, Y., et al., 2017a. Effect of refined waste and bio-based oil modifiers on rheological properties of asphalt binders. Construction and Building Materials 148, 504—511.

Zhang, R., Wang, H., Gao, J., et al., 2017a. High temperature performance of SBS modified bio-asphalt. Construction and Building Materials 144, 99—105.

Lorenzo Paolo Ingrassia is a PhD student at Università Politecnica delle Marche (Italy). His research is mainly focused on the application of renewable materials in asphalt pavements and on the tribological characterization of bituminous binders.

Gilda Ferrotti is an assistant professor of roads, railways and airports at Università Politecnica delle Marche (Italy). Dr. Ferrotti is involved in research activities mainly concerning reinforcement of flexible pavements, warm mix asphalt technologies, and innovative pavement materials. She has served as co-investigator in several international research projects and is author/coauthor of many scientific publications in the field of pavement engineering.

Xiaohu Lu is a senior technical specialist in Nynas and manages various research and development (R&D) projects on bitumen and bituminous materials. He has PhD in highway engineering from KTH Royal Institute of Technology in Stockholm, Sweden, and MSc and BSc degrees in chemistry from University of Science and Technology of China. Prior to joining Nynas in 2002, he was an associate professor at KTH. Xiaohu Lu is a member of the Association of Asphalt Paving Technologists (AAPT), and a senior member of RILEM and serves at different technical committees.

Francesco Canestrari is a full professor of roads, railways and airports and chair of the master degree in civil engineering at Università Politecnica delle Marche (Italy). Professor Canestrari is involved as principal investigator in several international research projects. His specialty areas include testing specifications, interface shear characterisation of asphalt layers, reinforced pavements, rheological and performance-based characterisation of sustainable and innovative pavement materials.